Dynamic Topology Optimization for Assuring Connectivity in Multihop Mobile Optical Wireless Communications Networks

Anurag Dwivedi, Paramasiviah Harshavardhana, Paul G. Velez, and Daniel J. Tebben

Mobile free-space optical links suffer from frequent link blockages because of opaque obstructions or link degradations, resulting in degraded or failed networks. We present a dynamic layer 1-based topology and routing control methodology for assuring connectivity in networks with fragile links. We describe core components of this methodology, with special emphasis on the dynamic topology optimization algorithm and topology transition schemes. The effectiveness of the proposed methodology depends on the fragility of the links compared with the topology optimization duration. If the link fragility is comparable to the time taken to achieve the optimal topology, then this methodology will not lead to a stable network. For this reason, the frequency and duration of link blockages are characterized for realistic terrains by using modeling and emulation tools incorporating the dynamic network changes experienced in theater networks. Link fragility results for various types of terrain suggest that the expected link longevity is significantly greater than the time taken by the proposed dynamic network optimization scheme. Thus, network connectivity can be greatly improved by using the proposed dynamic topology control methodology and optimization of physical network parameters such as antenna height.

INTRODUCTION

Background

Free-space optical (FSO) communication technology is advancing quickly, with recent field demonstrations of 80 Gbps for more than 100 km of range.[1] A few critical challenges still remain[2,3] pertaining to scintillation-, turbulence-, and weather-related link degradation, complete link blockage, and mobility of the platforms.

Mobile FSO and directional RF technology is developing rapidly,[4–6] paving the way for future deployments of mobile directional mesh networks or directional mobile ad hoc networks (MANETs).

The directional nature of an FSO network makes it particularly useful in environments where high bandwidth, low bit error ratio, low probability of intercept, and low probability of detection are important. FSO and directional RF networks offer the promise of higher network capacities compared with omnidirectional MANETs, but they have the drawback of increased link fragility. By link fragility we mean the tendency of a link to go up and down because of a variety of factors, such as

- Scintillation, turbulence, and fading
- Terrain- and structure-induced blocking
- Jamming
- Nonpermissive operational environment and concerns for signal detection or interception where radio powers may intentionally be lowered, turned off, or pointed in a different direction
- Mobility and resulting dynamic topology changes
- Pointing, acquisition, and tracking error
- Spectrum unavailability and inability to reuse spectrum
- Link degradation because of weather, foliage, and other obstructions
- Lack of interoperability with waveforms and radios on other platforms
- Battery life

As a consequence, directional mobile networks face a number of challenges at the physical layer. To provide reliable network support, MANETs must provide fast restoration mechanisms that confer a certain measure of reliability on the network.

A significant amount of effort has been devoted to developing protocols and algorithms for MANETs,[7] primarily focusing on restoration at the Network Layer (layer 3) of the Open Systems Interconnection (OSI) stack. These layer 3 MANET approaches make the fundamental assumption that a physical network will be available to provide suitable paths for traversing datagrams or packets and focus on providing Internet Protocol layer-recovery mechanisms to restore communications in the event of a failure. There are two main drawbacks to layer 3-based MANET restoration approaches: (*i*) they are too slow to prevent significant loss of traffic and will not be suitable for a net-centric operations environment, which relies on near 100% network availability, and (*ii*) they are inefficient in the sense that they attempt to find a layer 3 solution to what is fundamentally a physical layer (layer 1 of the OSI stack) problem.

In this article, we argue that FSO and directional RF wireless networks must address the topology and routing control problem at the physical layer, layer 1 of the OSI stack, and must do so in such a manner that layer 1 restoration is achieved without layer 3 becoming aware of the fact that a layer 1 failure occurred. Such an approach is reasonable because the link fragility in mobile wireless networks results mainly from physical phenomena such as scintillation, fading, and link blockages that directly affect the physical layer links. Recovery from such failures can best be achieved using dynamic physical topology optimization and control in response to or in anticipation of physical failure conditions. In this article, a dynamic network optimization methodology is presented on the basis of the hypothesis that assured connectivity can be achieved if a persistent, dynamic, and transparently controlled physical topology can be offered to the higher layers (such as layer 3).

Adaptive Networking Framework

MANETs may operate in a wide variety of conditions that support widely differing network connectivities. At one extreme, only intermittent connectivity between a subset of nodes may be possible because of prevailing conditions. At another extreme, a fairly reliable physical infrastructure may exist with only occasional disruptions because of node or link failures. The dynamic nature of mobile wireless networks, and the wide range of operating conditions, makes the networks unpredictable from a topology perspective, requiring an adaptive networking approach as suggested in Ref. 8. Depending on the physical networking resources available at each node, various network connectivity scenarios may be possible, such as a full physical mesh, full logical mesh, mesh enabled by timeshared links, and disruption/delay-tolerant networks,[9,10] where connectivity may be infrequent and sporadic.

For each of these scenarios, an optimal set of algorithms and protocols can be designed to maximize the performance within the constraints of that particular scenario. As a result, it may be necessary to adaptively and dynamically select a set of algorithms and protocols for ensuring the best performance of the applications supported by a mobile wireless network.

Basic steps in the adaptive networking framework are described in Fig. 1. The first step is to characterize the network scenario. This may include finding the node density, node degree, mobility, terrain, link fragility, traffic demand between node pairs, and other physical parameters. On the basis of these parameters and with the help of simulation and emulation tools, the type of scenario can be characterized. On the basis of the network scenario, an adaptive suite of algorithms, protocols, and cross-layer interactions can be selected (the second step in Fig. 1) for the network or subnetwork. Once the scenario type is characterized and the protocol suite is selected, network formation, dynamic control, and man-

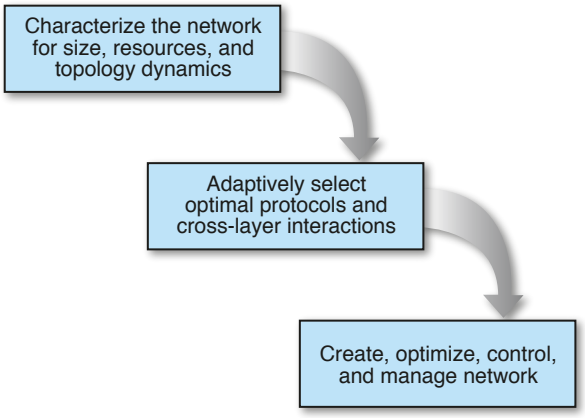

Figure 1. Steps in adaptive mobile wireless network formation.

agement methodology are determined to maintain the best possible topology for the specific network scenarios and applications (third step in Fig. 1).

Although maintaining a full physical layer mesh in a directional MANET is impractical, especially for a large network, the goal of a dynamically optimized full logical layer 1 mesh is achievable with multiple redundant paths for each node pair and is the main goal of the research described in this article.

In the past several years, there have been a number of studies devoted to layer 1 restoration schemes for tackling the challenges described earlier.[11–14] These approaches are based on centralized control and management and focus on specific topologies,[11,14] the availability of special network management nodes,[12] or traffic flow optimization.[13] A fundamental problem with centralized control approaches is that they rely on the availability of a "master" node to perform the critical topology and route calculations in response to network changes and then to relay the topology and route updates to all the network nodes. The problem of how to deal with the loss of the master node is a very significant one and has not been addressed effectively in any of these studies.

In contrast to the approaches described in Refs. 11–14, the approach we take in this article is to formulate the topology, traffic, and routing problem as a joint optimization problem. The solution to this problem simultaneously yields a robust topology, maximizes traffic flow, and allows for traffic priorities to be explicitly incorporated into making topology and routing decisions. A key advantage of this approach is that it does not rely on a master node, but rather all nodes in the network participate as equals. Every node performs the same distributed calculations, which converge very fast (on the order of tens of milliseconds on laptop processors available in 2007, for networks with a few tens of nodes) and produce a robust "near optimal" solution. Typical commercially available processors would suffice for performing the topology and route update calculations. Just as in the other approaches described in Refs. 11, 12, 14, and 15, here too we assume the existence of a signaling network that provides network status information to all the MANET nodes. Such network status information would typically be provided via link state update messages being transmitted by every node to its neighboring nodes periodically (on the order of tens of milliseconds in the MANET environment) or whenever there is an event trigger. An example of an event trigger would be a change in link availability or a significant change in link cost (which itself would be a composite of several factors such as link blocking, attenuation, traffic volume, priority of traffic, etc.).

Specific algorithms and schemes for dynamic topology optimization are described in this article. A modeling and simulation platform is described to create and visualize the scenarios, estimate expected longevity of the MANET topology, evaluate physical network performance, and quantify the effectiveness of the dynamic topology optimization and transition algorithms for maintaining a full logical mesh. Characterization is done for a variety of terrains including mountains, hills, valleys, and flat land, with five different locations of each type. Link fragility analysis is performed to assess the feasibility of the dynamic topology control schemes suggested.

METHODOLOGY FOR ASSURING PHYSICAL LAYER CONNECTIVITY BY MAINTAINING A FULL LOGICAL MESH

The approach suggested in this article attempts to compute topologies with multiple restoration paths between all communicating node pairs at all times. Physical layer connectivity, either single-hop or multihop, is assured between every node pair by dynamically optimizing the topology and maximizing the number of node- and link-disjoint paths between every node pair (two paths are link disjoint if they have no common link; similarly, two paths are node disjoint if they have no common node). Having multiple restoration paths allows communication to be maintained between various node pairs for longer durations and extends the lifespan of a deployed topology. This approach reduces the need for frequent topology optimization events, thus minimizing traffic disruptions caused by topology redeployment in mobile networks. Key components of this methodology are presented in Fig. 2 and are summarized below.

Network Discovery

Network discovery and network awareness messaging is the first required step in this methodology (Fig. 2). This step identifies various communicating nodes that

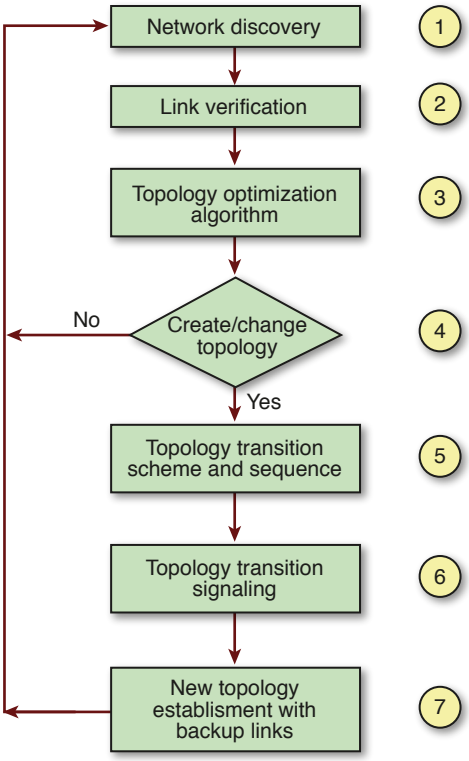

Figure 2. Illustration of the dynamic topology optimization methodology.

are to be joined as a network as well as the current link and node state of every node in the network. This mechanism is used to communicate network awareness messages between the network nodes and includes information on mobility, location, RF radio and FSO transmission characteristics, available transceivers or apertures, available and used wavelengths, available and used ports, remaining fuel and battery power, local weather conditions, link performance data and quality of service, current and requested traffic load, and possibly other data needed for predictive topology optimization.

Several potential approaches for discovery and control signaling may be used, including an RF or optical search with beacon signal[16] or an in-band or out-of-band omnidirectional RF control channel for node and link state broadcast.

In all of these approaches, a new node joining a MANET needs to identify itself to at least one of the networked nodes. After the credentials are verified, a node is authenticated to join the network using predefined protocols and policies.

Link Verification

For directional links such as FSO, the connectivity with in-range nodes cannot be predicted. This is because two nodes, despite being within range, may not be in the direct line of sight (LOS) of each other. For this reason, the next step in the topology control methodology (Fig. 2) is to verify the link between node pairs.

Link verification can be achieved by using a dedicated transceiver on each node for this purpose, or any available transceiver can be used opportunistically for this purpose. Alternatively, a video or static camera can be used with image recognition technology to determine the LOS. Periodic LOS or link verification data can then be broadcast through the discovery or network awareness signaling. Each node will locally maintain a list of neighboring nodes that are within range and have one or more LOS transceiver pairs available for forming links.

Topology Optimization Algorithm

This is a key process step for forming a directional mesh and requires careful choice of algorithms and protocols. Because of the link fragility of tactical communication links, it is recommended that multiple pre-computed restoration paths be determined and, if possible, pre-provisioned, to provide the desired restoration agility and network robustness. Desired characteristics of the optimization algorithm include the following.

- The algorithm should provide distributed control and management with uniform methodology and algorithms used by all nodes yielding the same optimal solution and enabling the application of uniform topology-forming policies throughout the network. This will ensure that every node in the network has the exact same topology and traffic information and will thus take actions consistent with those taken by other nodes. Of course, supervisory control signals can be exchanged between nodes via the omnidirectional network to confirm that all nodes have the same topology and traffic information.

- The algorithm should incorporate a network cost (objective function) measure that characterizes the chosen topology and helps in determining the trigger or threshold for topology change in order to better adapt to the prevailing networking scenario and environment.

- For dynamic networks, fast convergence meeting an acceptable network cost threshold is more important than obtaining a global minimum cost solution. An efficient algorithm with fast (no more than a few tens of milliseconds) convergence with acceptable initial network cost is sufficient. Once an acceptable topology is implemented, the algorithm should strive to improve the optimization in a stepwise fashion to bring the cost closer to a global minimum for implementation at a future transition event. Such an approach will allow meeting the fast convergence requirement while using affordable commercial off-

the-shelf processors with low cost, space, weight, and power.

- The algorithm should provide topology optimization using predictive parameters for enhanced robustness. Predictive capability can be enabled by prerecorded and real-time databases with tactical information provided by the network awareness signaling including basic node and link state information, weather, blocking, speed, mobility, and terrain information.
- The algorithm should include an optimal topology control scheme that strives for maximum network robustness and minimal disruption during topology transition; the scheme should be adaptable with tunable cost parameters.

An algorithm meeting these requirements has been developed and is described in detail in the *Topology Transition* section.

Decision to Change the Topology

When the differential between the current network cost and the best computed topology cost becomes large enough, the decision engine is prompted to change the topology (Fig. 3). The decision policies to change the topology must be developed carefully because the change will likely involve deliberately breaking some links and forming new ones to improve the overall network performance and robustness. However, in this process the traffic traversing the affected links will be interrupted, and this may affect the performance of the supported applications negatively. The need for topology optimization to enhance robustness needs to be balanced with the desire for link and topology longevity and good performance of the applications being supported. Other factors determining the topology transition decision include availability of predictive network awareness data, link fragility, network dynamics, mobility, and the ability of the applications to recover from lost packets.

Timescales of link fragility and mobility and the formation time for new topology are key factors in deciding the frequency of migration to an enhanced topology. In order for the network to remain within some threshold of variance from the true instantaneous optimum, the algorithm convergence and reconfiguration times need to be substantially smaller than the link fragility. This can be expressed by the inequality below:

$$t_{\text{discovery}} + t_{\text{convergence}} + t_{\text{PA}} + t_{\text{transition}} + t_{\text{OH}} < t_{\text{topology longevity}}, \quad (1)$$

where $t_{\text{discovery}}$ is the time taken for network awareness signaling and for link verification and $t_{\text{convergence}}$ is the time it takes for the topology optimization algorithm to determine the near optimum topology at a given instant. Parameter t_{PA} is the time required for pointing and acquisition, $t_{\text{transition}}$ is the time to complete the topology transition, and t_{OH} is the control overhead time. Parameter $t_{\text{topology longevity}}$ is the average time for which a deployed topology remains usable. The duration for which a topology is usable is a function of both the link fragility and the availability of back-up paths. The question of when a deployed topology stops being usable and needs to be updated is a rather complex one and is discussed in detail, along with a method for transitioning from the deployed topology to a new topology, in the *Topology Transition* section. The time required for the topology transition to occur after the threshold has been crossed is determined by the new link acquisition time and overhead time. Because analytic determination of link and topology longevity does not appear tractable, a simulation-based analysis is performed as described in the *Summary, Conclusions, and Future Work* section.

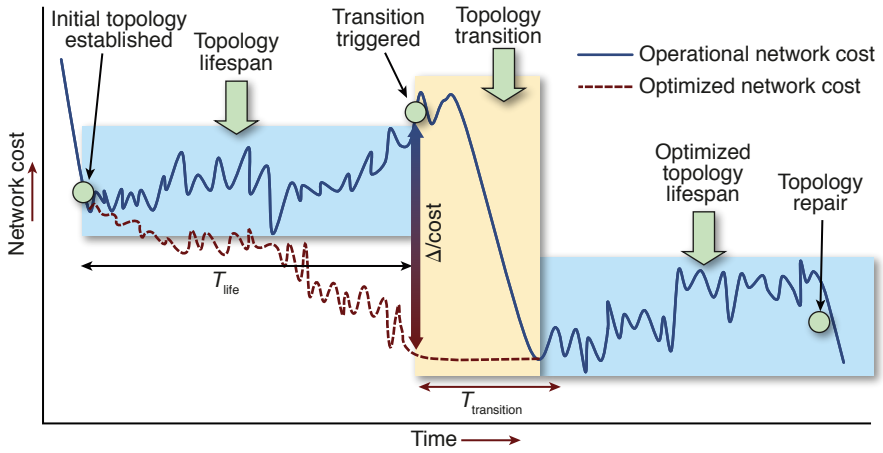

Figure 3. Persistent topology optimization and decision for topology transition. Solid and broken lines indicate the current network and optimized network costs, respectively.

Topology Transition Scheme

The topology transition process requires complex algorithms to determine the sequence of links to disconnect and form if a decision to migrate to a new topology has been made at step 4 of Fig. 2. This is generally a more complex problem than it seems at first glance. The main requirement is to achieve a smooth and agile transition that results in minimal disruption to existing traffic. In this article, we present and analyze a promising approach to topology transition.

Signaling and Link Establishment

Once the topology transition sequence has been determined, the new transceiver pairs prepare to form a new link. This includes breaking the existing link, notifying the network and higher layers of the broken and new links, and exchanging handshake messages to form the new link.

It is assumed that the sequencing scheme will establish a set of links to allow provisioning of primary paths carrying live traffic first and then establish the remaining links to allow the provisioning of non-traffic-carrying links and the secondary and higher-order restoration paths. The establishment of links supporting the restoration paths will, in general, be done using the same methods used by primary link formation.

The link establishment step involves pointing and tracking, adjusting transceiver compatibility, invoking performance monitoring of the link, and optimizing link quality. When the new transceiver pairs establish a stable link they communicate the new link information to the network and to the control and management planes of the higher layers.

When optical paths between two nodes are not possible, the system can be designed to automatically offer either a directional RF- or omnidirectional RF-based communication mechanism. This requires sophisticated cross-layer interaction for data pruning, compression, and priority-based policies because the drop in service bandwidth will be drastic when transitioning from optical- to RF-based communication.[17]

LINK FRAGILITY MODELING AND SIMULATION

For the proposed assured connectivity methodology to work, the topology longevity should be long enough to allow the completion of all process steps described in Fig. 2 before the topology degrades significantly. If links break too often for the topology optimization process to keep up, the optimization algorithm will not be able to converge and the network will become unstable. For the network scenarios of interest, a link fragility analysis needs to be performed to determine whether the optimization algorithm can converge fast enough and whether the deployed topology can be maintained for a reasonable duration before degrading below a threshold level. A simulation-based study using the Tactical Edge Network Emulation Tool (TENET) has been conducted to gain insights into these issues and is described briefly below.

An Overview of TENET

TENET is a modeling and simulation tool developed in MATLAB for the purpose of evaluating tactical networks in a dynamic, realistic tactical environment. The key features of TENET are given below and are explained in detail elsewhere.[18]

TENET is designed to provide physical layer metrics based on user-definable scenario parameters. The model is used for wireless signals that require LOS connections, such as free-space optical or directional RF signals. Through a user-friendly graphical user interface, simple or complex scenarios can be defined, modified, visualized, and evaluated for physical layer network performance.

The input parameters to the tool are the terrain, mobility, radio characteristics, and node types. The user can also model specific physical layer topology algorithms and specify link capacities. The terrain is based on Digital Terrain Elevation Data (DTED).[19] When available, databases of buildings can also be included in the terrain model for more realistic LOS modeling. The LOS calculations are performed for each node pair having compatible radios, and the overall connectivity is then estimated. The connectivity in this tool is defined as the ratio between the number of node pairs that have an end-to-end communication path and the number of node pairs desiring to communicate. If nodes contain radios capable of performing a relay function then an end-to-end path may contain multiple hops.

Because a tactical network is mobile and dynamic, a single connectivity snapshot is not adequate when assessing the performance. TENET has two modes of operation for modeling the dynamic tactical network. The first mode allows analysis of random or user-defined network evolution resulting from specific mobility models. Several mobility models are available. In each case, the speed and altitude of the node is defined, either for individual nodes or groups of nodes, and the connectivity is calculated as the nodes move through the scenario. In this time-based methodology, a view of how the network progresses over time is determined and can be clearly visualized. The second mode allows the analysis of statistical ensembles of static network topologies.[20] In this mode, a Monte Carlo simulation is used for a random laydown of nodes for each iteration of the simulation. Average network performance is evaluated for a particular environment with a particular set of nodes. It is especially useful when the number and types of nodes is known but the exact locations, mobility, or paths of the nodes are not well defined. Nodes can be confined to specific areas to represent a mission focus.

In both of the operational modes of TENET, the impact of node degree on LOS connectivity can be modeled. Topology optimization algorithms can be used to determine the most efficient and robust topology when node degrees (number of physical links incident on a node) are constrained to 2, 3, 4, or 5 for participating nodes.

Besides connectivity, TENET tracks several other statistics about the network performance. These include link throughput, number of hops, and link fragility and longevity. Clearly, links in a very rough terrain will break more often compared with the links in a smooth terrain.

The related metric of link downtime provides estimates of the duration for which a link remains broken once it breaks. This metric only tracks the downtime of links that had first been connected.

TENET-based results are used in this article to generate average link fragility in the scenarios of interest and eventually to determine the feasibility of the proposed assured connectivity methodology.

Characterizing Link Fragility in Dynamic Networks Using TENET

For characterizing the link fragility of directional networks in mountains, hills, valleys, and flat terrain, five different regions were selected for each type of terrain, as shown in Table 1. Each region extended over 50 × 50 km square in TENET simulations. Terrain was based on DTED-1 (~100 × 100 m resolution map).[19]

For each of the 20 geographical regions, the network characterization including connectivity and link fragility analysis was performed for four specific operational cases of node laydown and mobility:

- Case 1: 20 ground nodes with repeated random laydown
- Case 2: 18 ground nodes and 2 air nodes with repeated random laydown
- Case 3: 20 ground nodes with constrained random walk motion (30 km/h)
- Case 4: 18 ground nodes and 2 air nodes with constrained random walk motion (30 km/h) for ground nodes and elliptical orbit for airborne nodes (250 km/h)

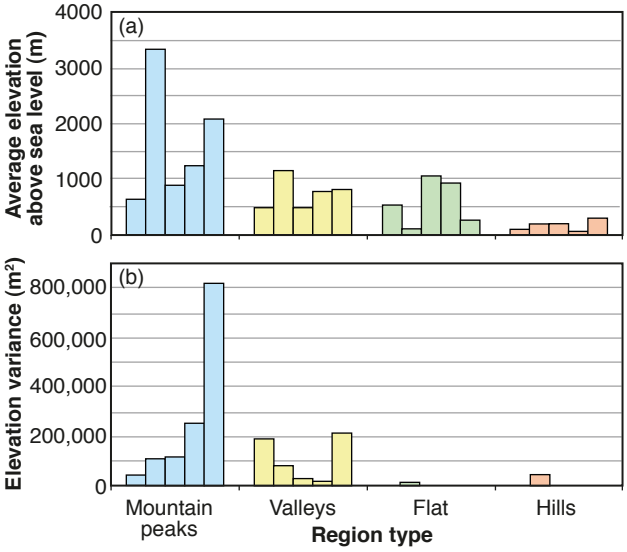

Figure 4. Average elevation above sea level (a) and elevation variance (b) for each of the 20 regions selected for this study.

For all of these cases, the node degree constraint was completely relaxed and connectivity was determined based on the LOS between node pairs. For the ground nodes, the antenna height was set at 3 m. Airborne nodes are moving at an altitude of 2000 m.

The regions were characterized on the basis of the profile of elevation above sea level, elevation variation, and slope variation of the terrain. Figure 4a shows the average elevation (in meters) above sea level for all of the 20 regions studied.

Severity of the terrain from the perspective of LOS blockage of directional beams is characterized by the elevation and slope variance within each region. The

Table 1. Description of 20 geographical locations selected for network and link fragility characterization.

Region type	Mean count
Mountain peaks	Mount Elbert, Colorado (N 38°50′32″, W 106°49′38″ and N 39°17′34″, W 106°14′50″)
	Mount Marcy, New York (N 43°53′23″, W 74°13′58″ and N 44°20′23″, W 73°36′19″)
	Clingman's Dome, North Carolina (N 35°20′14″, W 83°46′29″ and N 35°47′16″, W 83°13′17″)
	Mount McKinley, Alaska (N 62°50′33″, W 151°30′3″ and N 63°17′39″, W 150°30′21″)
	Mount Rainier, Washington (N 46°37′40″, W 122°5′16″ and N 47°4′40″, W 121°25′47″)
Valleys	Great Rift Valley, Jordon/Israel (N 30°3′35″, E 34°58′20″ and N 30°30′35″, E 35°29′34″)
	Glacier National Park, Montana (N 48°7′7″, W 114°38′23″ and N 48°34′11″, W 113°57′44″)
	Lexington, Virginia (N 37°33′44″, W 79°43′25″ and N 38°0′46″, W 79°9′14″)
	Ward Cove, Virginia (N 36°47′52″, W 81°56′59″ and N 37°14′56″, W 81°23′7″)
	Parkdale, Oregon (N 45°18′1″, W 121°54′59″ and N 45°45′1″, W 121°16′26″)
Flat	Somalia, Africa (N 8°29′16″, E 47°40′25″ and N 8°56′19″, E 48°7′47″)
	Baja California, Mexico (N 27°9′10″, W 113°43′20″ and N 27°36′13″, W 113°12′53″)
	Colorado/Kansas (N 38°1′53″, W 101°55′4″ and N 38°28′56″, W 101°20′41″)
	Southwestern Afghanistan (N 29°51′44″, E 64°28′56″ and N 30°18′44″, E 65°0′10″)
	Central Australia (S 27°57′53″, E 133°20′16″ and S 27°30′50″, E 133°50′50″)

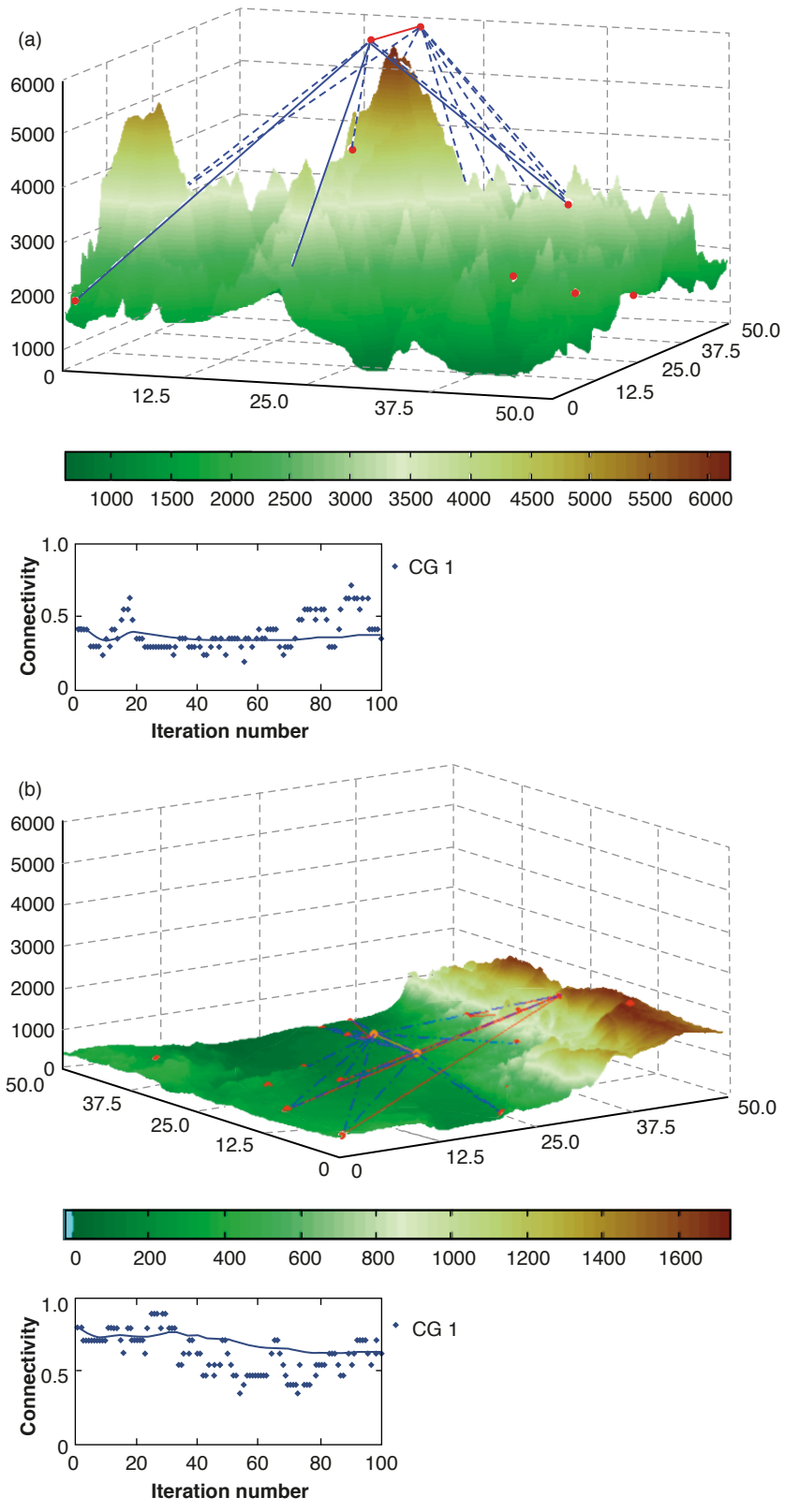

Figure 5. Examples of a mountain terrain in Mount McKinley, Alaska (50 km × 50 km) (a), and a valley terrain in the Great Rift Valley, Jordon/Israel (50 km × 50 km) (b), and network scenarios, as well as the dynamic connectivity results. Horizontal axes on the terrain visualization windows are in kilometers, and vertical axes are in meters.

elevation variance for all of these 20 regions is plotted in Fig. 4b. As expected, the variance for the flat regions is low compared with mountains and valleys.

Examples of two of the four terrain types are shown in Fig. 5 (horizontal axes on the terrain visualization window are in kilometers and the vertical axes are in meters). For each of these examples, there are 18 ground nodes and 2 airborne nodes with mobility parameters as defined in the operational case 4 above. Overall connectivity is estimated as a function of time (in arbitrary units or a.u.) and is plotted below the terrain and network visualization window for each case. Connectivity here is defined as the fraction of node pairs having at least one working communications path between them. It varies between 0 and 1, with 0 indicating no connectivity between any pair of nodes and 1 indicating 100% connectivity between every pair of nodes having at least one path between them. Final average connectivity reported in Fig. 6 is the average over 100 iterations for all four cases described above. Figure 6 has 20 bars describing average connectivity for each of the 20 regions selected.

As expected, the average connectivity for the flat land is found to be the highest, at approximately 64%. For this study, the connectivity is defined as: connectivity = (number of node pairs having at least one available path/total number of node pairs). Or, for a network with n nodes, connectivity is defined as: connectivity = [number of node pairs having at least one available path/$0.5(n^2 - n)$].

The mesh network analysis performed here assumes that multihop connectivity is feasible between two nodes and, therefore, permits multihop paths to be established between node pairs. Across all the node pairs, the average number of hops is estimated to be less than 2 and the average of the maximum number of hops ranges from 3.75 (for flat terrain) to

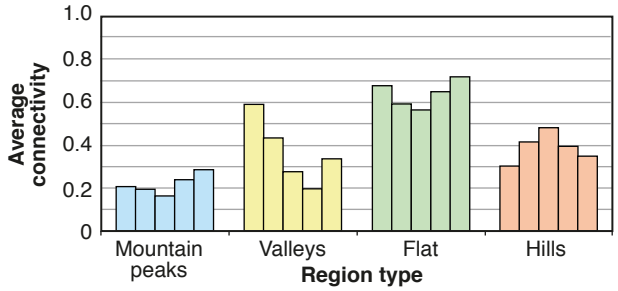

Figure 6. Average connectivity for each of the 20 regions selected for the study.

6.50 (for mountain terrain). This information may be useful in specifying the worst-case requirements from link budget or end-to-end delay perspectives.

Link longevity is reported in Fig. 7. For each of the 20 regions selected, Fig. 7a shows the results of average duration for which a link remains down because of the LOS blockages. Interestingly, this study shows that for the scenario chosen, the links are blocked for a significant period of time, i.e., ranging, on average, from 180 s to approximately 540 s.

This has major implications for the design of mobile networking protocols. With outages on the order of 180–540 s, most end–end sessions will time out. This would mean, for example, that a layer 3-based restoration will have to first time out to recognize a link failure and then find alternate routes dynamically for the affected traffic. Physical layer restoration approaches such as the one we present would, on the other hand, react to the link blockage event within several tens to several hundreds of milliseconds (depending on the thresholds chosen) and switch the traffic to an alternate path well before the end–end sessions time out. The performance of protocols designed for fixed infrastructure may be significantly impacted if used unaltered for these mobile conditions.

Another implication of the link downtime finding is that if a topology degrades because of link blockages, the links cannot be relied upon to restore themselves naturally and the layer must be restored physically. Otherwise, the performance of protocols and applications will suffer unless they can tolerate several hundred seconds of delay.

Another significant finding of this work is average link uptime, as shown in Fig. 7b. It is important to know the average uptime to determine the topology update frequency and the effectiveness of the topology optimization protocol. As described in Fig. 3 and Expression 1, if the topology is highly dynamic and if the links are highly fragile, dynamic topology control may not be feasible. This is because there is a finite length of time required for topology discovery, optimization algorithm convergence, topology transition, signaling, and other overhead functions. If the topology is highly dynamic, the dynamic optimization process may not be able to keep up with the link fragility, and the optimized topology may become stale even before being implemented.

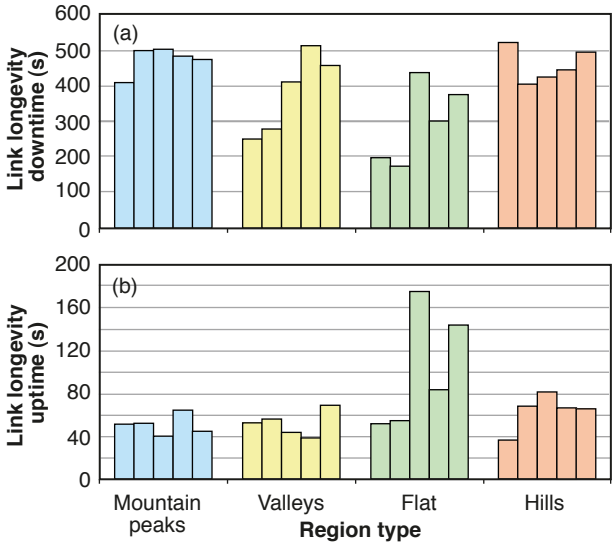

Figure 7. Average link longevity downtime (a) and uptime (b) for each region.

Figure 7b shows that although the link longevity is shorter than the average time a link is down, it is still long enough to implement dynamic topology optimization of the physical mesh, since our topology optimization algorithm achieves convergence in less than 100 ms. On average, the link longevity is found to be approximately 40 s or better. For flat land it reached as high has 170 s for the scenarios tested in this study. These results neglect foliage and other man-made objects not included in the terrain DTED data. Also, weather conditions are assumed to provide a radio range of 100 km.

Link fragility and longevity estimated from this analysis will be compared with topology convergence and time required to complete other processes of the suggested methodology to determine the viability of the approach.

OVERVIEW OF DISTRIBUTED ADAPTIVE PRECOMPUTED RESTORATION ALGORITHM

Central to the proposed methodology is a new distributed adaptive precomputed restoration (DAPR) algorithm[21] for achieving fast layer 1 restoration. A brief overview of the algorithm will be presented here. DAPR adapts to changes in the MANET backbone topology by quickly computing topology and route updates. There are several salient characteristics of DAPR. First, it allows one to choose a suitable network graph; in this article, we have presented results that are based on a graph that ensures three diverse paths (one primary and two or more backup paths) between every node pair. Second, DAPR is adaptive and responds automatically

to the changes in topology because of loss of links and/or nodes. Third, it is distributed in nature, which means the need for a master node is obviated; every MANET node runs the algorithm independently and converges to the same topology and routing. Last, it utilizes arbitrary link cost functions which may include link performance parameters such as blocking, attenuation, and available bandwidth; traffic parameters such as traffic volume to be carried and traffic priority; penalty factors to force certain high-priority links to be included in the topology; and any other cost parameters that are deemed to be desirable. Any of these can be included in the link cost function without any significant impact on algorithm convergence.

As mentioned earlier, the DAPR paradigm assumes the existence of a signaling network that conveys topology update messages to all MANET nodes either periodically on the basis of preset timers or following certain event triggers, such as the onset of certain failure conditions or exceeding network availability thresholds. The update message includes information on all possible link connections a node can establish with its neighboring nodes, along with a link metric measuring the quality of each link. DAPR uses a simulated annealing-based optimization procedure to determine the best possible layer 1 connectivity and the corresponding layer 1 routing.

The DAPR algorithm has two distinct and separable components: the topology update component and the route update component. The topology update component focuses on realizing any desired preselected network graph, such as, for example, a ring or a star, using the best available physical (layer 1) links as measured by the most recent link metrics received via the topology update message. In other words, during each topology update interval, the topology update algorithm uses the most recent layer 1 link and node information available to determine the best possible way to construct the desired layer 1 network graph. Once the best topology conforming to the preselected network graph is determined, a predetermined routing pattern for the network graph is computed and the new layer 1 routes are then invoked. If the network graph is chosen appropriately, the layer 1 route computation procedure can be dramatically simplified. The particular network graph we have used for the studies presented in this article is well known in communications network literature and has several optimal properties. We will describe this network graph later. It must be emphasized, however, that the DAPR approach will work with any preselected network graph. For example, the generalized Moore graphs used in Ref. 13 may be used if they offer more desirable routing and reliability properties. The topology update component incorporates traffic considerations via the link metric and, hence, the simulated annealing formulation actually solves a joint topology and traffic flow optimization problem.

The topology update component of DAPR is formulated as a mathematical optimization problem. As mentioned earlier, the topology update component requires that the desired network topology (ring, star, mesh, etc.) be first specified. Let $\mathbf{X}(i,j)$ be the adjacency matrix of the graph corresponding to the desired network topology. Let $\mathbf{C}(i,j)$ be the cost matrix specifying the cost of connecting node i to node j. The cost representation is completely general and may include components corresponding to the MANET technology, distance between nodes, the traffic to be carried on a given link, the robustness of a given link or node, traffic priority, etc. The cost matrix is updated during each topology update interval by using a link state protocol that allows nodes to exchange the most recent link cost information with their neighbors. This allows each node in the MANET to maintain the current version of the cost matrix **C** which, in essence, represents the current MANET state reflecting the dynamics of mobility, blockage, link and node availability, the traffic to be carried, etc.

Let the MANET have n nodes, $N_1, N_2, N_3, \ldots, N_n$. Then **X** and **C** are $n \times n$ matrices. A fundamental observation in the DAPR algorithm is the following. For the given network graph with the adjacency matrix represented by **X**, we have the freedom of assigning physical MANET nodes $N_1, N_2, N_3, \ldots, N_n$ to the network vertices $1, 2, 3, \ldots, n$. Each separate assignment of physical nodes to network vertices generates a different topology with different link connectivities but the same underlying logical network graph (ring, star, mesh, etc.). Thus, by changing the assignment, we can produce different network connectivities that support the desired type of physical layer robustness. For example, by choosing a ring graph, we can ensure network connectivity of degree two supporting two diverse paths between every node pair. For the assignment that assigns nodes $N_1, N_2, N_3, \ldots, N_n$ to network vertices $1, 2, 3, \ldots, n$, it can be shown through some simple matrix algebra[22] that the total network cost is ½ **Trace** (**XC**), where **Trace** is the standard matrix function corresponding to the sum of diagonal elements.

By applying a permutation transformation **R** (a transformation represented by an identity matrix whose rows have been interchanged), one may change the connectivity between the MANET nodes while maintaining the network topology. The permutation transformation, in essence, changes the order in which the nodes are connected but maintains the prescribed topology. Under the permutation transformation, the new adjacency matrix is given by $\mathbf{R}^{-1}\mathbf{X}\mathbf{R}$ and the corresponding cost matrix is given by $\mathbf{R}\mathbf{C}\mathbf{R}^{-1}$. It can be shown that the corresponding total network cost is given by ½ **Trace** ($\mathbf{X}\,\mathbf{R}\mathbf{C}\mathbf{R}^{-1}$) (see Ref. 22 for details). During each topology update interval one may attempt to find the optimal MANET connectivity that minimizes the total network cost. This may be formulated as the problem of finding

the permutation transformation **R** that minimizes the total MANET cost, i.e., minimize **Trace** (**X RCR**$^{-1}$) over all possible permutation transformations **R**.

Figure 8b shows the three possible unique network node assignments for this graph.

To illustrate these points let us consider the following simple example. Let a MANET have three physical nodes located in New York (NY), Los Angeles (LA), and New Jersey (NJ). Let the logical network graph chosen be a tree. Let the cost matrix be the distance matrix, i.e., the matrix whose entries represent the distance between the nodes. Figure 8a shows the graph and the **X** and **C** matrices. Figure 8b shows the three node assignments and the corresponding costs. It is clear from this example that different node assignments produce different network costs, and there is an assignment (not necessarily unique) that produces the minimum network cost.

For reasons of brevity, we have not provided details of the mathematical formulation, which can be found in Refs. 21 and 22. This optimization problem is a mixed-integer programming problem that is NP-complete and cannot be solved exactly for realistic network sizes. It is in fact a generalization of the familiar traveling salesman problem. If we choose the ring graph, it reduces to the standard traveling salesman problem. The optimization problem is amenable to a simulated annealing-based solution. Our novel mathematical formulation allows us to exploit certain matrix structures within the permutation transformation, allowing the simulated annealing cost function to be updated without intensive numerical computations. This, in turn, affords very fast convergence, on the order of tens of milliseconds, for realistic MANET sizes of several tens of nodes. This allows this protocol to be used in a battlefield MANET environment where the network nodes and links are expected to change rapidly. One of the key flexibilities afforded by DAPR is the fact that the cost function that drives the simulated annealing algorithm may be customized by the user to reflect nuances of a specific MANET technology, the peculiarities in traffic patterns, or any other chosen network characteristic. As will be seen later, the customizability of the cost function allows us to introduce certain topology transition penalty functions that enable smooth transition from the deployed DAPR network to the newly computed network.

As mentioned earlier, the DAPR protocol can be implemented for any chosen network graph. The topology transition results discussed in subsequent sections are with reference to a specific network graph we have chosen for its optimal routing properties. For details of the graph itself, we refer the reader to Ref. 22. The graph is illustrated for a six-node MANET in Fig. 9.

The main properties of this graph, of interest from the network availability perspective, are that the graph provides the maximum number of edge- and node-disjoint paths between all node pairs, with the minimum possible links; that for the specific case of a degree 3 graph, it provides three diverse paths between all node pairs; and that the three paths may be used as the primary path and secondary and tertiary backup paths, with the end–end route trivially computed via table lookups with minimal computational burden. The three diverse paths between nodes 1 and 4 are illustrated in Fig. 9. The fast route computation coupled with the fast topology convergence enables DAPR to be used in realistic MANET environments.

Simulation studies of DAPR show that this protocol affords significant improvements in network availability under realistic mobile conditions and demonstrates fast topology and route convergence, on the order of 100 ms, for a network with tens of nodes.

TOPOLOGY TRANSITION

Transition Schemes

An approach for minimal traffic disruption during topology transition must be developed for high-availability tactical networks such as a tactical backbone that provides bandwidth service to the higher layers.

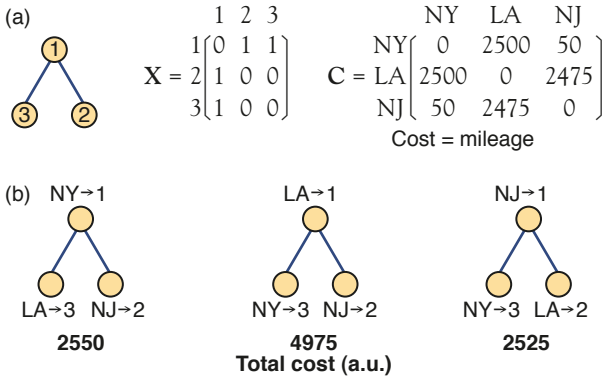

Figure 8. An example graph (a) and an example graph with different node assignments (b).

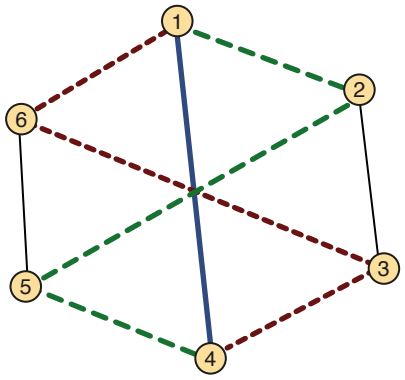

Figure 9. Robust network graph used in DAPR. The three diverse paths between nodes 1 and 4 are shown.

Topology transition is a complex problem. Several approaches can be envisioned for topology transition as discussed below.

Brute Force Approach

This approach relies on breaking all the links that need rearrangement and recreating the new topology without regard to the impact on the traffic being carried. This approach is least complex but has the maximum negative impact on the users supported by the network. A more desirable goal, however, would be to provide a graceful topology transition with minimum disruption to the existing traffic.

Embedded Transition Tree Approach

This approach ensures the availability of a transition tree that is common to both the deployed network graph and the newly computed graph, as shown in Fig. 10. This approach will be explored in greater detail in this section.

In this approach, traffic is temporarily moved on to transition paths computed from the embedded transition tree while newly optimized links/paths are being constructed. Once the optimized links/paths are available, the traffic is transferred from the transition paths to the new optimal paths. Some traffic may be minimally impacted in switching to the transition tree from the deployed topology and then again when switching from the transition tree to the newly computed topology.

Integrated Transition Scheme

This is a conceptually sophisticated control plane scheme that attempts to directly integrate the transition needs into the topology computation step. Whether this can be accomplished or not is a subject for further research.

Overview of the Embedded Transition Tree Approach

As shown in Fig. 10, the main idea in the embedded transition tree approach consists of ensuring that the currently deployed topology and the newly computed topology have at least one tree in common. If such a common tree can be ensured, then new end-to-end paths can be computed between all node pairs (or only those with live traffic), and the traffic can be switched over to the new paths. The deployed topology can then be rolled over to the newly computed topology. Because live traffic is being carried on tree links that are common to the two topologies, there should be minimal disruption. Thus, this approach supports hitless transition. The network load during the transition period will be limited by the capacity of the tree branch with the highest utilization. In order to accommodate additional flows, multiple embedded transition trees may be needed. But those scenarios are beyond the scope of this article.

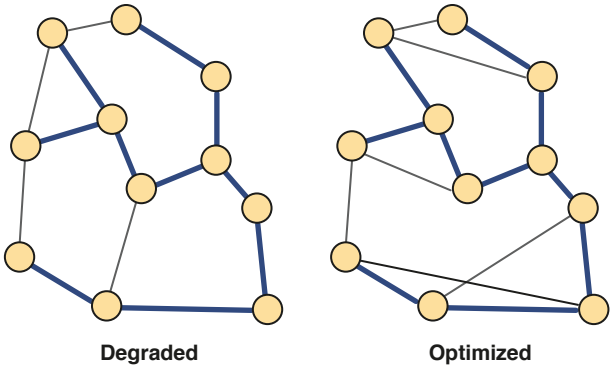

Figure 10. Embedded transition tree approach. Common transition tree is indicated by thick blue lines.

We conducted an extensive simulation study to determine the feasibility of this approach. Below we present the results from the simulation study.

Simulation Results for the Embedded Transition Tree Approach

We begin by giving a brief overview of the simulated annealing-based optimization that computes new DAPR graphs. At the starting time t_0, a DAPR graph is computed by using simulated annealing based on the link cost metrics. Details of the simulated annealing procedure may be found in Refs. 21 and 22. For simplicity, here we use a uniform link cost of 100 for feasible links and a very large number (representing infinity) for infeasible links. Once a new DAPR graph is computed, the corresponding network cost is calculated. If the new cost is less than the old cost, the new DAPR iteration is accepted as an improvement. If the new cost is greater than the old cost, then the new graph is accepted with a certain probability depending on the cooling temperature, as per standard practice in simulated annealing. Once all the simulated annealing iterations are executed, or the freezing condition is reached, the lowest cost DAPR graph computed is accepted as the "optimal" solution. The corresponding topology is then deployed. At subsequent topology update intervals, T_i, every node in the network runs the simulated annealing algorithm with updated cost metrics to determine the best new DAPR graph.

We enhance the fundamental simulated annealing approach to ensure that embedded transition trees are available. The basic idea is to add a transition tree penalty to the simulated annealing cost described earlier. It should be emphasized again here that we are exploiting the flexibility in the simulated annealing approach to add cost penalties as desired. We first compute a set of spanning trees within the deployed DAPR graph, called TS_{deployed}. During each simulated annealing iteration, we compute TS_{deployed} for the candidate DAPR graph.

We then check to see if there exists a tree, T, within $TS_{deployed}$ that has all links in common with the candidate DAPR graph. If such a tree is found, then the transition tree penalty associated with that DAPR graph is 0. If no common tree exists, then a transition tree penalty is added on to the newly computed network cost. The transition tree penalty, T_{cost}, is computed as $T_{cost} = 1{,}000{,}000 \times n_{missing}/n_s$, where n_s is the number of links in the spanning tree T_s belonging to $TS_{deployed}$ and $n_{missing}$ is the number of links missing between T_s and the candidate DAPR graph.

It can be seen that the penalty T_{cost} severely penalizes a newly computed DAPR graph that has even a single tree link missing; this ensures that any DAPR graph chosen will have a common transition tree as long as such a tree is feasible in the sense that such a tree can be constructed from the available links.

We further introduce the notion of a path cost to determine when a newly computed DAPR network topology should be accepted in preference to the currently deployed DAPR topology. The path cost is computed as $Path_{cost}$ = sum over all node pairs $\{(0.6 \times (1- P_1) + 0.3 \times (1- P_2) + 0.1 \times (1- P_3) + 10 \times (1- P_1) \times (1- P_2) + 100 \times (1- P_1) \times (1- P_2) \times (1- P_3)\}$, where $P_1 = 1$ if the primary path between a node pair is available, otherwise it is 0; $P_2 = 1$ if the secondary path between a node pair is available, otherwise it is 0; and $P_3 = 1$ if the tertiary path between a node pair is available, otherwise it is 0. It is easy to see that the $Path_{cost}$ metric is a measure of the connectivity and robustness of the topology. Because the DAPR graph chosen for this study (Fig. 9) supports three diverse paths between every node pair, the path cost function defined as above penalizes a graph heavily if all three paths between a node pair are unavailable.

We accept a newly computed DAPR topology if the new $Path_{cost}$ is less than the $Path_{cost}$ of the deployed DAPR topology by at least 10. A path cost differential of 10 is chosen as the acceptance threshold because it indicates that either at least one node pair has all three paths unavailable or that several node pairs have multiple unavailable paths; either is enough to warrant concern about the robustness of the topology. The new DAPR topology is then "deployed," and the simulated annealing runs continue. It should be noted that the penalty $Path_{cost}$ is not a component of the simulated annealing cost and is used only for making topology acceptance decisions. Before we present the simulation results, we first define some network measures.

- **Network cost:** This is the cost metric that is used for driving the simulated annealing-based optimization. It consists of three components: (*i*) the node degree penalty, which is 10,000 for every node having a degree of 0, 1,000 for every node having a degree of 1, 100 for every node having a degree of 2, and 0 for every node having a degree of 3; (*ii*) the transition tree penalty T_{cost} defined earlier; and (*iii*) the sum of all the link costs, where link costs are chosen to reflect the specific directional MANET technology being used, the traffic being carried, the distance between node pairs and other factors as described in Refs. 21 and 22. In this study, link costs are chosen to be 100 if a link is feasible and a very large number (infinity) if it is not. It should be noted that the various penalty numbers were chosen in this research effort on the basis of trial and error; however, a methodology for specifying penalty can be matured during final protocol design for operational implementation of this approach.
- **Average node degree:** average over all network nodes of the individual node degrees
- **Average connectivity:** percentage of node pairs with at least one available path between them; it is a measure of the overall connectivity in the network
- **Number of transitions:** the number of times the newly computed DAPR topology was accepted on the basis of the $Path_{cost}$ metric within a run of 100 topology update intervals where a new DAPR topology is computed in each interval

We begin our discussion of simulation results with a discussion of the number of transitions. In order to see how many valid transitions would be available on the basis of the path cost metric, we ran a simulation of accepted transitions for different networking scenarios. To illustrate, we show a 30-node network scenario (24 ground nodes and 6 airborne nodes) in Fig. 11. Figure 12 plots the number of transitions for networks of 10, 20, and 40 nodes using realistic terrain data with mobility, blocking, and link fragility models. The three networks included two, five, and eight unmanned aerial vehicles (UAVs), respectively, for providing better LOS connectivity. The UAV nodes had a maximum altitude of 500 m. Each node used a random walk mobility model with an antenna height of 3 m and a maximum range of 7 km. DTED data for the Middle Eastern region were used to generate a 10 × 10 km terrain model.

Looking at Fig. 12, it is clear that a significant number of transition opportunities are available beyond a transition tree set size of four. The fact that the number of transitions does not go up monotonically with the number of spanning trees is at first glance surprising. The relationship between the number of transitions and the number of spanning trees is quite complex because it also depends on the quality of the currently deployed topology and the extent to which the deployed topology has deteriorated because of changing network conditions. As one increases the number of spanning trees, the likelihood of a high-quality solution that supports smooth transition being available increases, and, thus,

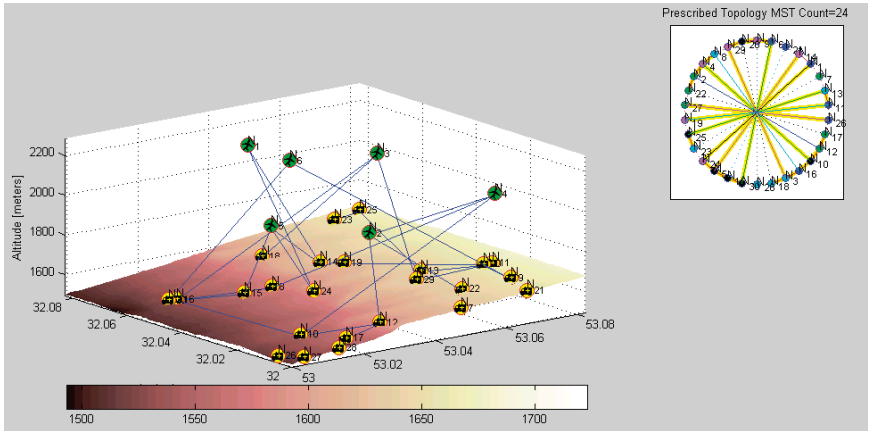

Figure 11. A scenario with 24 ground nodes and 6 airborne nodes used for testing the embedded tree-based topology transition scheme. MST, minimum spanning tree.

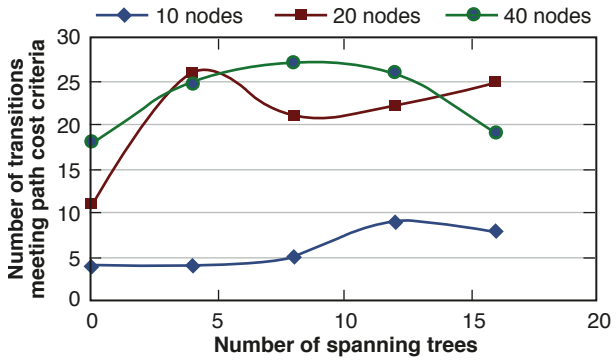

Figure 12. Number of transitions that meet the $Path_{cost}$ metric within the 100 DAPR computation iterations.

the probability of improving upon it decreases, which explains why the graph dips in all cases. However, this does not give a clear idea of the transition opportunities available compared with a deployed DAPR topology; this is because, in the above plots, once the new DAPR topology is accepted, a transition has already been made and the subsequent comparisons are with this "new" topology as the deployed topology. In reality, one would not be transitioning so frequently, since transition imposes other penalties as discussed earlier. The next question we set out to answer is how many transition opportunities can we expect over a time span during which a deployed DAPR topology may be expected to persist.

To do this, we ran the simulation for 1000 update intervals and computed the network metrics, without transitioning from the deployed DAPR topology to a newly computed DAPR topology. The network size consisted of 30 nodes, seven of which were UAVs. The UAV nodes had a maximum altitude of 500 m. Each node used a random walk mobility model with an antenna height of 3 m and a maximum range of 7 km. The Middle Eastern terrain model was used. The number of transitions is not computed because no transitions are allowed in this simulation scenario because the purpose was to evaluate how many potential transitions would be available over the expected topology longevity interval.

At each update interval we plot the network metrics for the deployed DAPR topology and the newly computed (but not accepted) DAPR topology; the plots representing these topologies are labeled deployed and transition, respectively, in Fig. 13.

The horizontal axes in Fig. 13 show the number of iterations or time in arbitrary units. The plots shown are for a network with 30 nodes; here the network cost is quite high and the average node degree and average network connectivity are significantly low, indicating that theater network conditions are quite harsh.

It can be seen that the embedded tree-based hitless transition topology curve is always significantly better for all metrics compared with the deployed topology curve. However, it does not generally perform as well as disruptive transition. A disruptive transition forms the new topology instantaneously without regard to traffic hit. For example, the average node degree frequently approaches 2.5 (maximum possible node degree is constrained to 3 for these scenarios) for the disruptive transition scheme (Fig. 13b), whereas it is significantly degraded for the deployed topology. Embedded tree transition scheme consistently improves the average node degree over the deployed topology, but not as well as seen in the case of disruptive transition. Disruptive transition should be viewed as an unrealizable upper bound because it does not take into account the effect of breaking existing traffic-carrying links.

Looking at Fig. 13c, we see that the average connectivity for the deployed topology starts at approximately 40% and deteriorates to approximately 15% toward the end of the simulation run. The average connectivity for the hitless transition topology starts at approximately 60%, rises to more than 80%, and stays at approximately 40% for the most part. The connectivity is less than 100% because of the mountainous terrain chosen. The $Path_{cost}$ plot in Fig. 13d shows that the $Path_{cost}$ remains very high for the deployed topology throughout the simulation interval, indicating that many node pairs have one or more unavailable paths; however, for the transition topology, there are several points at which the $Path_{cost}$ drops sharply, indicating these would have been suitable epochs for effecting a topology transition.

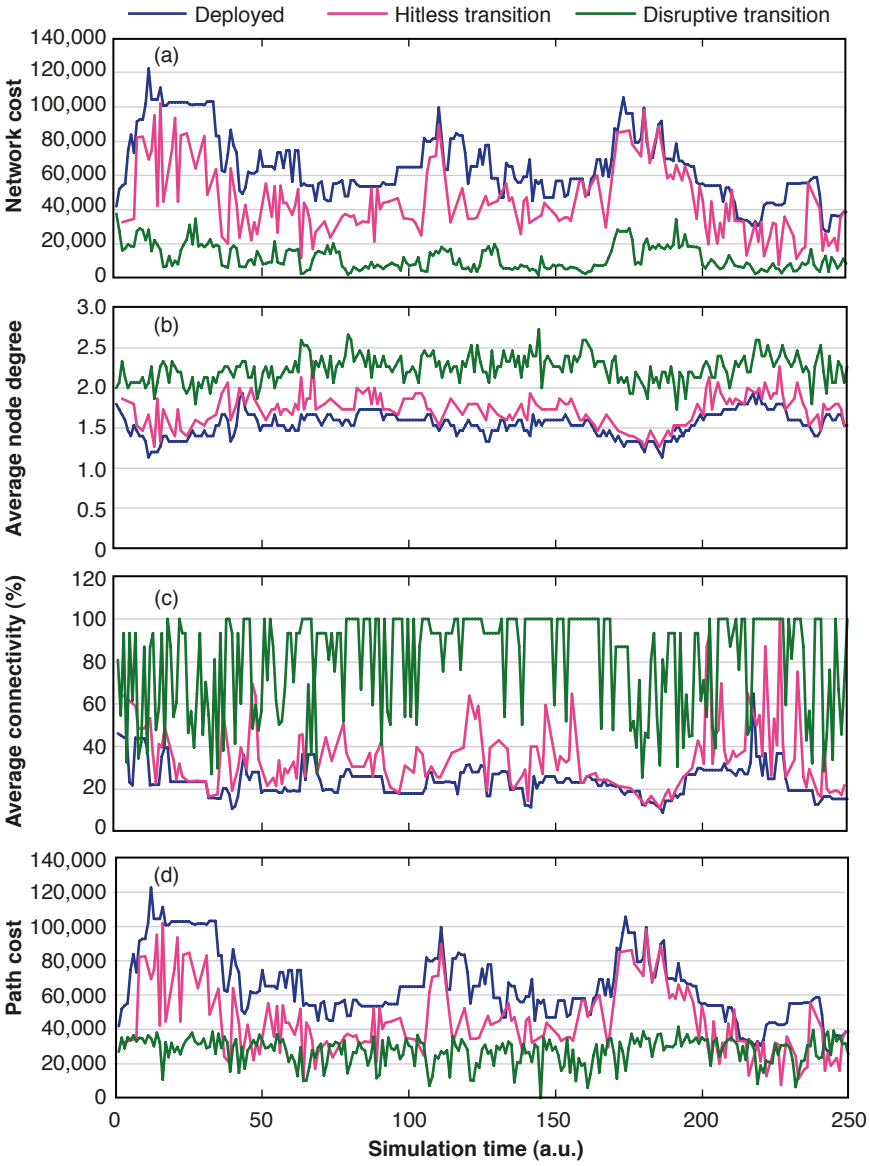

Figure 13. Network cost (a), node degree (b), average connectivity (c), and path cost (d) plots for deployed and possible transition topologies for a 30-node network over a realistic transition interval.

It should be emphasized that at every one of these potential transition epochs, a common transition tree was available to make possible a hitless transition, as can be seen from the network cost plot in Fig. 13a, which would have shown a very high cost value at these instants for the transition topology if it had not had a common transition tree available (because the transition tree penalty, T_{cost}, is very high).

These simulation results provide very significant support for the use of an embedded transition tree to enable hitless transition in DAPR-based MANETs. Furthermore, the results indicate that the notion of a $Path_{cost}$ is a very appropriate metric for triggering topology transitions. More work is needed to make the approach described here practical and field deployable. A very encouraging aspect of this approach is that it did not increase the simulated annealing convergence time to any significant extent.

SUMMARY, CONCLUSIONS, AND FUTURE WORK

Because tactical MANETs operate in widely differing network conditions, we propose an adaptive networking framework where every node is aware of the network topology through a network discovery protocol. On the basis of the network resources, node density, and performance requirements, a decision is made to select the best combination of protocols for the MANET. This decision is implemented network-wide but in a distributed manner.

If there are sufficient resources to formulate and maintain a full logical mesh, a dynamic topology optimization and control methodology can be used, the details of which are described. Dynamic optimization of full logical mesh is possible if the link longevity is not too short. Network characterizations in diverse terrain were performed to estimate average link longevity. Results show that the average link uptime ranged from 40 to 170 s for the scenarios studied. This is longer than the estimated topology optimization cycle time, which is found to be less than 10 s. An estimate of 10 s for the topology optimization cycle is based on the existing technologies[1,4–6] and the assumption that each process step in Fig. 2 can be achieved in a few hundred milliseconds. However, a detailed study needs to be performed to further justify this assumption.

These results suggest that the overall topology optimization and transition time is substantially less that the average link longevity, supporting the possibility of sustained full logical mesh for directional RF and FSO networks. The article presented a DAPR scheme for performing topology and routing control at layer 1. It also presented an embedded tree-based topology transition approach that enables a hitless transition

from the currently deployed topology to the newly computed optimal topology. A cost measure is identified to alert when a topology transition should be initiated. Modeling and simulation results are presented to show that the embedded tree-based DAPR scheme achieves significant improvements over a static topology scheme and results in much better connectivity and overall network cost.

Future work will focus on enhancing topology longevity by performing local fixes to node and link failures and extending the DAPR graph used in this article to a family of graphs with similar routing properties that support multiple diverse paths between node pairs. This will substantially increase the DAPR search space and may further improve the quality of the solution found in each topology update interval. While making the adaptive network protocol selection (the second step in Fig. 1) it should be noted that DAPR generally is best suited to topologies with significant available node degree and does not perform as well in sparsely connected topologies. Thus, extending the DAPR approach to developing topology control algorithms for sparse networks is an important evolution. On the other hand, a mobile network can be designed to have assured connectivity using DAPR if sufficient networking assets are available or planned. We have performed a simulation-based study of the embedded transition tree approach and derived significant insights into the performance of this approach as well as the development of appropriate transition criteria. However, further research is needed to develop effective topology transition criteria to ensure that topology transition is triggered only when it results in significant improvement in network performance over the current topology. The topology transition scheme must also take into account wavelength reuse and contention.

ACKNOWLEDGMENTS: We thank Harrison Chao for helping with terrain analysis and the Infocentric Operations and Science and Technology business areas of APL for providing independent research and development funding for most of this work.

REFERENCES

[1]Young, D. W., Sluz, J. E., Juarez, J. C., Airola, M. B., Sova, R. M., et al., "Demonstration of High-Data-Rate Wavelength Division Multiplexed Transmission Over a 150 km Free Space Optical Link," in *Proc. SPIE Defense and Security Symp.*, Orlando, FL, paper 65780R (2007).

[2]Juarez, J. C., Dwivedi, A., Mammons, A. R., Jones, S. D., Weerackody, V., et al., "Free-Space Optical Communications for Next-Generation Military Networks," *IEEE Communications Magazine*, pp. 46–51 (Nov 2006).

[3]Dwivedi, A., "Critical Technology Gaps and Potential Solutions for Mobile Free Space Optical Networking," in *Proc. IEEE Military Communications Conf. (MILCOM)*, Piscataway, NJ, pp. 251–257 (2006).

[4]Sova, R. M., Sluz, J. E., Young, D. W., Juarez, J. C., Dwivedi, A., et al., "80 Gb/s Free-Space Optical Communication Demonstration Between an Aerostat and a Ground Terminal," in *Proc. SPIE Optics and Photonics Conf.*, San Diego, CA, paper 630414 (2006).

[5]L-3 Communications, *Multi-Role Tactical Common Data Link*, http://www.l-3com.com/csw/docs/MR-TCDL%20Product%20Line.pdf (accessed 19 May 2011).

[6]Harris Corporation, *HNW (Highband Networking Waveform)*, http://www.govcomm.harris.com/solutions/products/000056.asp (accessed 19 May 2011).

[7]Toh, C.-K., *Ad Hoc Mobile Wireless Networks: Protocol and Systems*, Prentice Hall, Upper Saddle River, NJ (2002).

[8]Dwivedi, A., Tebben, D. J., Paramasiviah, H., Hammons, A. R., and Nichols, R. A., "A Control Plane Architecture for Mobile Free Space Optical Network and Directional RF MANETs," in *Proc. IEEE Military Communications Conf. (MILCOM)*, Orlando, FL, pp. 1–7 (2007).

[9]Nichols, R. A., Hammons, A. R., Tebben, D. J., and Dwivedi, A., "Delay Tolerant Networking for Free-Space Optical Communication Systems," in *Proc. Sornoff Symp.*, Princeton, NJ, pp. 1–5 (2007).

[10]Nichols, R. A., and Hammons, A. R. Jr., "DTN-Based Free-Space Optical and Directional RF Networks," in *Proc. IEEE Military Communications Conf. (MILCOM)*, San Diego, CA, pp. 1–6 (2008).

[11]Milner, S. D., and Desai, A., "Autonomous Reconfiguration in Free-Space Optical Sensor Networks," *IEEE J. Sel. Areas Comm.* **23**(8), 1556–1563 (2005).

[12]Sun, F., and Shayman, M., "Local Restoration for Bandwidth Guaranteed Connections in Mobile Optical Backbone Networks," in *IEEE Wireless Communications and Networking Conf.*, New Orleans, LA, pp. 1749–1754 (2005).

[13]Guan, K., Ghanadan, R., McNeil, K., and Kumar, S., "Topology Formation for Tactical Networks with Directional RF and Free-Space Optical Links," in *Proc. IEEE Military Communications Conf. (MILCOM)*, San Diego, CA, pp. 1–7 (2008).

[14]Milner, S. D., and Davis, C. C., "Hybrid Free Space Optical/RF Networks for Tactical Operations," in *Proc. IEEE Military Communications Conf. (MILCOM)*, Monterey, CA, pp. 409–415 (2004).

[15]Ahn, G.-S., Campbell, A. T., Lee, S.-B., and Zhang, X., *INSIGNIA*, IETF Draft, Columbia University, http://tools.ietf.org/html/draft-ietf-manet-insignia-01 (Oct 1999).

[16]Hindman, C., and Robertson, L., "Beaconless Satellite Laser Acquisition—Modeling and Feasibility," in *Proc. IEEE Military Communications Conf. (MILCOM)*, Monterey, CA, pp. 41–47 (2004).

[17]Nichols, R. A., "Protocol Adaptation in Hybrid RF/Optical Wireless Networks," in *Proc. IEEE Military Communications Conf. (MILCOM)*, Atlantic City, NJ, pp. 1–7 (2005).

[18]Tebben, D., Dwivedi, A., Madsen, J., Turner, W., Garretson, J., et al., "TENET (Tactical Edge Network Emulation Tool): A Tool for Connectivity Analysis for Tactical Scenario," in *Proc. IEEE Military Communications Conf. (MILCOM)*, San Diego, CA, pp. 1–7 (2008).

[19]National Geospatial-Intelligence Agency, *Digital Terrain Elevation Data*, https://www1.nga.mil/ProductsServices/Topographical Terrestrial/DigitalTerrainElevationData/Pages/default.aspx (accessed 21 Jan 2011).

[20]Tebben, D., Kim, P. Y., and Dwivedi, A., "Tactical Network Connectivity Planning," in *Proc. IEEE Military Communications Conf. (MILCOM)*, Orlando, FL, pp. 1–7 (2007).

[21]Harshavardhana, P., Tebben, D. J., Dwivedi, A., and Hammons, A. R. Jr., "DAPR (Distributed Adaptive Precomputed Restoration): An Algorithm for Assured Availability Directional RF and FSO MANET," in *Proc. IEEE Military Communications Conf. (MILCOM)*, Orlando, FL, pp. 1–6 (2007).

[22]Harshavardhana, P., "Design and Analysis of Nonhierarchical Node-by-Node Routing Virtual Circuit Networks," in *Proc. IEEE Global Communications Conf. (GLOBECOM)*, Dallas, TX, pp. 1434–1439 (1989).

The Authors

Anurag Dwivedi

Paramasiviah Harshavardhana

Paul G. Velez

Daniel J. Tebben

Anurag Dwivedi is a member of APL's Senior Professional Staff, a Project Manager, and the Section Supervisor of the Directional Networks Section of the Applied Information Sciences Department. Dr. Dwivedi initiated dynamic topology control and network optimization research for wireless optical and directional RF networking systems at APL. Dr. Dwivedi architected the framework for optimizing tactical networks for assured connectivity, resiliency, and robustness. **Paramasiviah Harshavardhana** is the Group Supervisor of the Systems and Information Sciences research group in the Milton Eisenhower Research Center. Dr. Harshavardhana has extensive experience in the design and analysis of many types of communications networks. He developed the DAPR for agile topology optimization for tactical wireless networks and used simulated annealing-based optimization methodologies for identifying precomputed topologies for tactical networks. **Paul G. Velez** is a software engineer in APL's Applied Information Science Department. He developed software for modeling dynamic topology transition to verify the relative impacts of various topology transition techniques. **Daniel J. Tebben** is a member of APL's Senior Professional Staff and the Assistant Section Supervisor of the Directional Networks Section of the Communication and Networking Technology Group in the Applied Information Sciences Department. He developed the code for the TENET used for tactical network analysis and for evaluating the effectiveness of a variety of dynamic topology optimization schemes. For further information on the work reported here, contact Anurag Dwivedi. His e-mail address is anurag.dwivedi@jhuapl.edu.

The *Johns Hopkins APL Technical Digest* can be accessed electronically at **www.jhuapl.edu/techdigest**.